

Coulomb effects on the fundamental optical transition in semiconducting single-walled carbon nanotubes: Divergent behavior in the small-diameter limit

Masao Ichida,^{1,*} Shuhei Mizuno,¹ Yahachi Saito,² Hiromichi Kataura,³ Yohji Achiba,³
and Arao Nakamura^{1,†}

¹Center for Integrated Research in Science and Engineering, and Department of Crystalline Materials Science, Nagoya University,
Furo-cho, Chikusa-ku, Nagoya 464-8603, Japan

²Department of Electrical and Electronic Engineering, Mie University, Tsu 514-8507, Japan

³Faculty of Science, Tokyo Metropolitan University, 1-1 Minami-Ohsawa, Hachioji, Tokyo 192-0397, Japan

(Received 23 April 2002; published 18 June 2002)

We have experimentally investigated the diameter dependence of Coulomb effects on the optical transition in semiconducting single-walled carbon nanotubes. The absorption band due to the lowest band-to-band transition shifts to the higher-energy side compared to the transition energy calculated by a tight-binding model. The blueshift originating from the Coulomb effect increases with decreasing tube diameter d as $d^{-1.3}$. We have found that this dependence is attributed to both the increase of the band gap and the enhancement of the exciton binding energy with a decrease of the diameter.

DOI: 10.1103/PhysRevB.65.241407

PACS number(s): 78.67.Ch, 71.35.Cc, 73.22.-f

Much effort has been devoted to understanding Coulomb effects in one-dimensional (1D) systems and to elucidating the connection between the theoretical model and various quasi-1D real materials. Theoretical study revealed the effect of electron-electron repulsion in the ground-state properties, resulting in a Peierls instability of 1D electron-phonon systems.^{1,2} The long-range Coulomb interaction leading to the formation of excitons plays an important role in optical transitions of low-dimensional systems. In a theoretical calculation of 1D systems, one has to postulate a cutoff length in the 1D Coulomb potential because of its singular nature. The theoretical calculations have shown that the binding energy and the oscillator strength of the lowest excitons drastically increase as the cross-sectional size of a quasi-1D system is reduced.³⁻⁵

The fundamental electronic structure of single-walled carbon nanotubes (SWNT's) is regarded as a quasi-1D system because of the high aspect ratio (length/diameter) of a fundamental structure. The 1D band structure and the van Hove singularity (VHS) have been predicted by using a tight-binding model, and scanning tunneling microscopy/spectroscopy,^{6,7} resonant Raman scattering measurements,⁸⁻¹² and transport measurements¹³ have revealed the characteristic properties of the quasi-1D system. Electron correlation effects have been theoretically studied from different points of view, because they are expected to become important for small nanotubes. Short-range electron-electron interactions and screened long-range Coulomb effects were investigated for armchair nanotubes.¹⁴⁻¹⁷ Ando theoretically pointed out the importance of Coulomb effects on optical transitions of SWNT's.¹⁸ In our previous work, we reported that the fundamental absorption band in semiconducting SWNT's is located at the higher-energy side compared to the band-to-band transition energy calculated by a tight-binding model because of the Coulomb effect.¹⁹

As we can prepare SWNT's with various diameters, the SWNT is a suitable system to elucidate a dependence of long-range Coulomb interactions on a cross-sectional size of a real quasi-1D system. A variation of the tube diameters

leads to a change in distance between electrons as well as a change in tube curvature. In this paper, we experimentally investigate the role of Coulomb interaction on the optical transition and its dependence on the tube diameter ranging between 0.98 and 1.52 nm in SWNT's. We find that the Coulomb effects plays a crucial role for a SWNT with a small diameter, showing a divergent behavior.

SWNT's were prepared by both the laser vaporization method and the electric arc discharge method.^{9,20} The metal catalyzed carbon rod was settled in a quartz tube which was filled at 500 Torr Ar gas and heated at 1000 °C. The second harmonic of the Nd:YAG (yttrium aluminum garnet) laser pulse was focused on the carbon rod. The laser-vaporized carbon and catalyst finally became soot containing SWNT's and nanoparticles of the catalysts. SWNT's were produced by electric arc discharge between the catalyzed carbon anode and the pure carbon cathode in an atmosphere of 500-Torr He gas. SWNT's with various diameters were obtained by changing a He gas pressure. NiY, NiCo, RhPd, and RhPt were used as catalysts to produce SWNT's with different diameters. The soot obtained using NiY and NiCo was purified by reflux in H₂O₂. Thin-film samples for optical measurements were prepared by spraying SWNT's/ethanol suspension on a quartz substrate.

The mean diameter of SWNT's (d_{av}) was determined by either Raman-scattering measurement or transmission electron microscope (TEM). The sample with a mean diameter of 1.28 nm was directly determined by TEM. The diameter distribution was well reproduced by a Gauss function,¹⁹ and the mean diameter and standard deviation are 1.28 and 0.07 nm, respectively as listed in Table I. The mean diameters of the four samples were determined from Raman scattering measurements using the relationship between the radial breathing mode (RBM) frequency ν_{RBM} and the diameter d ($d = 248/\nu_{RBM}$).¹² To avoid a small deviation from the above relationship due to a resonant Raman effect, we used an incident light with the photon energy of 2.54 eV, because the resonant effect was suppressed for the incident light with a

TABLE I. The mean diameter (d_{av}) and standard deviation (σ) of the tube diameter distribution. The values were determined from Raman scattering (a), TEM (b), and fitting of absorption spectra (c). $\hbar\omega_{RBM}$ is the Raman frequency of the radial breathing mode.

Catalyst	d_{av} (nm)	σ (nm)	$\hbar\omega_{RBM}$ (cm ⁻¹)
RhPd	0.98 ± 0.04^a	0.11^c	252
NiCo	1.22 ± 0.04^a	0.07^c	204
RhPt	1.28 ± 0.07^b	0.07^b	–
NiCo	1.38 ± 0.04^a	0.07^c	180
NiY	1.52 ± 0.04^a	0.14^c	163

higher photon energy.²¹ For a photon energy of 2.40 eV the correction for diameter is estimated to be about 6% in the diameter range studied here. For the photon energy used in this study (2.54 eV), the correction is less than 6%.

The bundle effect of nanotubes also give a small shift of the RBM frequency.²¹ When the number N of tubes in a bundle is 10, the correction for diameter is estimated to be $\sim 5\%$ for 0.98 nm and $\sim 8\%$ for 1.52 nm using the result reported by Kuzmany *et al.*²¹ The correction due to this effect is comparable to that of the resonance effect. Since a value of N is not known for the samples used in this study, we do not take into account the bundle effect for a determination of the diameter. Although there remain uncertainties due to resonance and bundle effects in the determination of the diameter from the RBM frequency, the diameter can be determined within an accuracy of about 10%.

The solid curves in Fig. 1(a) show the absorption spectra of the SWNT film with a mean diameter of 1.22 nm measured at 4.2 and 300 K. Three broad absorption bands are

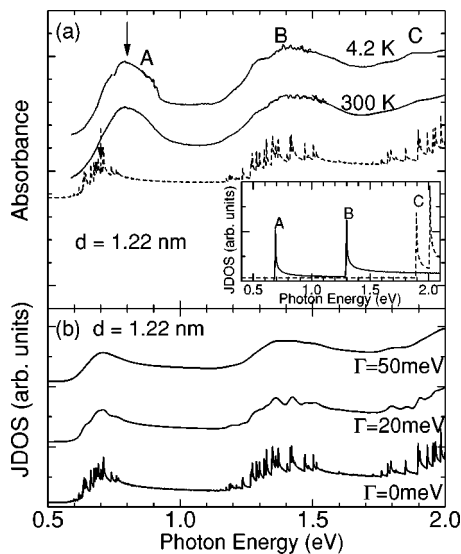


FIG. 1. (a) Absorption spectra of SWNT's with a mean tube diameter of 1.22 nm measured at 4.2 and 300 K. The broken curve is the averaged JDOS which is calculated by Eq. (1). The overlapping integral is 2.9 eV. Inset: JDOS of a SWNT with the chiral vectors of (15, 1) (solid curve) and (12, 6) (broken curve). (b) Calculated absorption spectra taking into account a diameter distribution with different values of spectral broadening Γ .

observed at ~ 0.8 eV (A), 1.4 eV (B), and 1.9 eV (C), and there is no significant difference between the spectra measured at these temperatures. The inset of Fig. 1 (a) shows the joint density of states (JDOS) for semiconducting (solid curve) and metallic (broken curve) SWNT's with a tube diameter of 1.22 nm. The JDOS was calculated by the simple zone folding model of the graphite band²² taking the nearest-neighbor carbon-carbon overlapping integral γ_0 to be 2.9 eV.^{8,12,21} In this band calculation, the Coulomb interaction is not taken into account.²² Sharp peaks appear at ~ 0.7 and 1.3 eV for the semiconducting tube and at ~ 1.9 and 2.0 eV for the metallic tube. Comparing the JDOS peaks with the observed spectra, the A and B bands are attributed to the optical transitions from the valence band to the conduction bands in semiconducting SWNT's, and band C is attributed to metallic SWNT's.^{9,19}

To discuss the spectral feature in more detail, we consider the diameter distribution because in the thin-film sample there exist various SWNT's with different chiral vectors (n_1, n_2). We calculate the averaged JDOS $D(E)$, taking into account a diameter distribution as

$$D(E) = \sum_{(n_1, n_2)} N(d_{(n_1, n_2)}) \rho_{(n_1, n_2)}(E), \quad (1)$$

where $N(d)$ is a diameter distribution function, and $d_{(n_1, n_2)}$ and $\rho_{(n_1, n_2)}(E)$ are a diameter and a JDOS for a SWNT with a chiral vector (n_1, n_2), respectively. The broken curve in Fig. 1(a) is the calculated result of Eq. (1) for $\gamma_0 = 2.9$ eV. We used the distribution function as a Gauss function with a mean diameter of 1.22 nm and a standard deviation of 0.07 nm. In the calculated JDOS, there are many small peaks corresponding to the VHS of an individual SWNT, but such small peaks are not seen in the observed spectra. In order to obtain a better fit of the observed spectra to the averaged JDOS, we introduce a broadening function of the JDOS. The absorption spectrum is given by

$$\alpha(E) = \int_0^\infty d\epsilon G(\epsilon) D(E - \epsilon), \quad (2)$$

where $G(\epsilon)$ is a spectral broadening function. Here we assume $G(\epsilon)$ to be a Gauss function which describes an inhomogeneous broadening of the optical transition. Shown in Fig. 1(b) are the calculated spectra for different values of a full width at half-maximum Γ of the Gauss function. With increasing Γ the calculated JDOS becomes broad and featureless, and the calculation for $\Gamma = 50$ meV can be compared to the observed spectrum. Here we note that the spectral position of the calculated JDOS agrees well with the observed absorption band B, but band A (indicated by solid arrow) is located at the higher-energy side by ~ 0.1 eV compared to the calculated energy (by broken arrow). Such a blueshift is ascribed to the Coulomb effect on the fundamental optical transition.^{18,19}

Now let us investigate the diameter dependence of Coulomb effects, measuring the absorption spectra of SWNT's with various mean diameters. The solid curves in Fig. 2 show the absorption spectra of SWNT films with different diam-

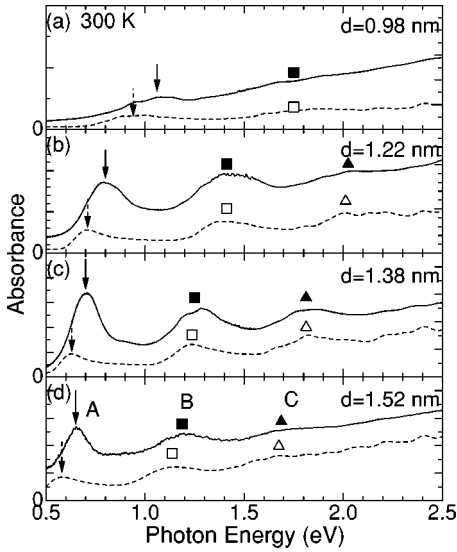


FIG. 2. Absorption spectra of SWNT's with different mean tube diameters d_{av} (solid curves) and calculated absorption spectra taking into account of diameter distribution of SWNT's (broken curve). The spectral broadening Γ is 50 meV. Solid and broken arrows show peak positions of fundamental absorption bands in the observed and calculated spectra, respectively. Squares and triangles are the peak energies of the B and C bands.

eters in the range of 0.98–1.52 nm. The peak energies of the A, B, and C bands depend on the mean diameters, and shift to the lower-energy side with increasing diameter from 0.98 to 1.52 nm. The broken curves in Fig. 2 display the calculated absorption spectra using Eq. (2) with $\Gamma = 50$ meV. The values of the mean diameters and the standard deviation used are listed in Table I. Comparing the calculated and observed spectra, the B- and C-band peaks (solid squares and open squares, and solid triangles and open triangles) agree well with the calculation, while the A-band peak (indicated by solid arrow) is located at the higher-energy side compared to the calculation for all the samples. A small shift observed in the B band for $d_{av} = 1.52$ nm is within the error in the diameter determination.

In Fig. 3 we plot the observed peak energies E^{obs} for the A, B, and C bands as a function of diameter by closed circles (A), closed squares (B), and closed triangles (C). The peak energy decreases with increasing diameter. Small dots in Fig. 3 display the calculated transition energy E^0 for each chiral SWNT in the diameter range of 0.85–1.55 nm, and the energy is approximately proportional to d^{-1} . The peak energies E^{calc} calculated using Eqs. (1) and (2) are shown by open circles in Fig. 3. E^{calc} is also proportional to d_{av}^{-1} , and is slightly higher than E^0 (small dots) because the JDOS of each chiral SWNT shows a tail at the higher-energy side of the VHS, as shown in the inset of Fig. 1. The blueshift due to this effect was pointed out by Margulis and Gaiduk²³ In our result, however, the A-band peak energy is higher than E^{calc} which is calculated taking into account the JDOS, and the B and C peak energies are in good agreement with the calculation. Therefore, the blueshift from E^{calc} observed for the A band indicates a Coulomb effect in the fundamental optical transition.

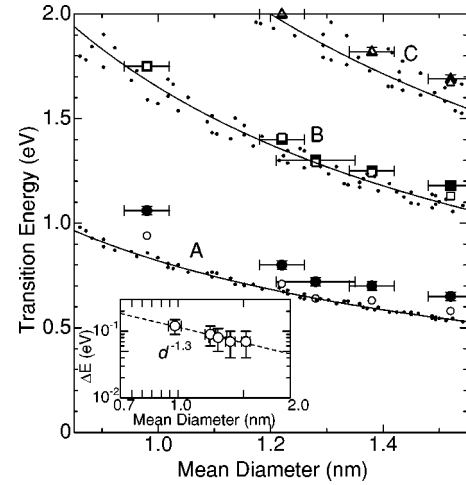


FIG. 3. Observed peak energies of the A band (closed circles), the B band (closed squares), and the C band (closed triangles) as functions of the mean tube diameter. The calculated peak energies are shown by open circles, open squares, and open triangles. The diameter dependence of energy separations between van Hove singularities is shown by small dots. Inset: the difference energy between the observed and calculated peak energies of the A band. The dashed line indicates the $d_{av}^{-1.3}$ dependence.

Let us discuss in detail the diameter dependence of the Coulomb interaction observed for the A band. The transition energy of the A band is written by

$$E_A^{obs} = E_A^{calc} + \delta E_G^{Coul} - \Delta E_B, \quad (3)$$

where E_A^{calc} is the band-gap energy calculated using the tight-binding approximation without Coulomb interaction, and $\delta E_G^{Coul} (>0)$ and $\Delta E_B (>0)$ are the component of the band gap increase due to the Coulomb interaction and the exciton binding energy, respectively. The strength of the Coulomb interaction is given by the energy difference $\Delta E = E_A^{obs} - E_A^{calc} = \delta E_G^{Coul} - \Delta E_B$. The observed variation of ΔE with tube diameter is shown by open circles in the inset of Fig. 3. The observed dependence indicates that the Coulomb interaction becomes stronger for small d , and the least-squares fit yields the dependence of $d_{av}^{-1.3}$. As shown by the theoretical study,¹⁸ both the energy of the continuum state (band gap) and the binding energy increase with increasing Coulomb energy. As a result, the lowest exciton energy is shifted to the higher-energy side compared to the transition energy without Coulomb interaction. Assuming a correspondence between the Coulomb energy and the diameter, the observed diameter dependence of the Coulomb effect can be attributed both the increase of the band gap (δE_G^{Coul}) and the enhancement of the binding energy (ΔE_B) with a decrease of the diameter. Considering the real situation of a SWNT, however, we point out that the shape is not stringlike but cylinderlike. In the smaller diameter tube below ~ 1.0 nm, the σ orbital is hybridized with the π orbital, and thus the curvature effect strongly modifies the electronic structure.²⁴ A full theoretical calculation of optical transitions taking into account both the

Coulomb and the curvature effects in SWNT's, is necessary to explain the observed diameter dependence of fundamental transition energies.

In conclusion, we have investigated the role of Coulomb interaction in optical transitions of SWNT's with different mean diameters in the range 0.98–1.52 nm. A comparison of the experiment and the tight-binding calculation has shown the blueshift of the lowest band-to-band transition depending on the diameter. It is found that the Coulomb interaction in SWNT's causes both an increase of the band gap and an enhancement of the exciton binding energy, and the diameter

dependence of the overall Coulomb effect is $d^{-1.3}$. In addition, such a Coulomb effect plays a key role in only the lowest optical transition, and disappears in the higher optical transitions associated with the second and third conduction and valence bands.

The authors would like to thank to Dr. H. Ajiki for useful comments and discussion. This work was supported by a Grant-in-Aid for Scientific Research (C) from the Japan Society for the Promotion of Science.

*Present address: PRESTO, JST, and Department of Physics, Faculty of Science and Engineering, Konan University, Okamoto 8-9-1, Higashi Nada-ku, Kobe 658-8501, Japan. Email address: ichida@konan-u.ac.jp

†Email address: nakamura@cirse.nagoya-u.ac.jp

¹S. Mazumdar and S.N. Dixit, *Phys. Rev. Lett.* **51**, 292 (1983).

²J.E. Hirsch, *Phys. Rev. Lett.* **51**, 296 (1983).

³M. Shinada and S. Sugano, *J. Phys. Soc. Jpn.* **21**, 1936 (1966).

⁴R.J. Elliot and R. Loudon, *J. Phys. Chem. Solids* **15**, 196 (1960).

⁵T. Ogawa and T. Takagahara, *Phys. Rev. B* **43**, 14 325 (1991).

⁶J.W.G. Wildöer, L.C. Venema, A.G. Rinzler, R.E. Smalley, and C. Dekker, *Nature (London)* **391**, 59 (1998).

⁷T.W. Odom, J.L. Huang, P. Kim, and C.M. Lieber, *Nature (London)* **391**, 62 (1998).

⁸M.A. Pimenta, A. Marucci, S.A. Empedocles, M.G. Bawendi, E.B. Hanlon, A.M. Rao, P.C. Eklund, R.E. Smalley, G. Dresselhaus, and M.S. Dresselhaus, *Phys. Rev. B* **58**, R16 016 (1998).

⁹H. Kataura, Y. Kumazawa, Y. Maniwa, I. Umezumi, S. Suzuki, Y. Ohtsuka, and Y. Achiba, *Synth. Met.* **103**, 2555 (1999).

¹⁰M. Milner, J. Kürti, M. Hulman, and H. Kuzmany, *Phys. Rev. Lett.* **84**, 1324 (2000).

¹¹M. Hulman, W. Plank, and H. Kuzmany, *Phys. Rev. B* **63**, 081406 (2001).

¹²A. Jorio, R. Saito, J.H. Hafner, C.M. Lieber, M. Hunter, T. Mc-

Clure, G. Dresselhaus, and M.S. Dresselhaus, *Phys. Rev. Lett.* **86**, 1118 (2001).

¹³M. Bockrath, D.H. Cobden, J. Lu, A.G. Rinzler, R.E. Smalley, L. Balents, and P.L. McEuen, *Nature (London)* **397**, 598 (1999).

¹⁴L. Balents and M.P.A. Fisher, *Phys. Rev. B* **55**, R11 973 (1997).

¹⁵Y.A. Krotov, D.-H. Lee, and S.G. Louie, *Phys. Rev. Lett.* **78**, 4245 (1997).

¹⁶R. Egger and A.O. Gogolin, *Phys. Rev. Lett.* **79**, 5082 (1997).

¹⁷C. Kane, L. Balents, and M.P.A. Fisher, *Phys. Rev. Lett.* **79**, 5086 (1997).

¹⁸T. Ando, *J. Phys. Soc. Jpn.* **66**, 1066 (1997).

¹⁹M. Ichida, S. Mizuno, Y. Tani, Y. Saito, and A. Nakamura, *J. Phys. Soc. Jpn.* **68**, 3131 (1999).

²⁰Y. Saito, Y. Tani, N. Miyagawa, K. Mitsushima, A. Kasuya, and Y. Nishina, *Chem. Phys. Lett.* **294**, 593 (1998).

²¹H. Kuzmany, W. Plank, M. Hulman, C. Kramberger, A. Gruneis, T. Pichler, H. Peterlik, H. Kataura, and Y. Achiba, *Eur. Phys. J. B* **22**, 307 (2001).

²²R. Saito, M. Fujita, G. Dresselhaus, and S. Dresselhaus, *Appl. Phys. Lett.* **60**, 2204 (1992).

²³V.A. Margulis and E.A. Gaiduk, *Phys. Lett. A* **281**, 52 (2001).

²⁴X. Blase, L.X. Benedict, E.L. Shirley, and S.G. Louie, *Phys. Rev. Lett.* **72**, 1878 (1994).